TISSUE ENGINEERING: Part A
Volume 19, Numbers 17 and 18, 2013

DOI: 10.1089/ten.tea.2012.0057

Guided Bone Regeneration in Long-Bone Defects with a Structural Hydroxyapatite Graft and Collagen Membrane

Teja Guda, PhD,[1,2] John A. Walker, MD,[1] Brian M. Singleton, BS,[2] Jesus W. Hernandez, BS,[2] Jun-Sik Son, PhD,[3,4] Su-Gwan Kim, DDS,[3,4] Daniel S. Oh, PhD,[5] Mark R. Appleford, PhD,[2] Joo L. Ong, PhD,[2] and Joseph C. Wenke, PhD[1]

There are few synthetic graft alternatives to treat large long-bone defects resulting from trauma or disease that do not incorporate osteogenic or osteoinductive factors. The aim of this study was to test the additional benefit of including a permeable collagen membrane guide in conjunction with a preformed porous hydroxyapatite bone graft to serve as an improved osteoconductive scaffold for bone regeneration. A 10-mm-segmental long-bone defect model in the rabbit radius was used. The hydroxyapatite scaffolds alone or with a collagen wrap were compared as experimental treatment groups to an empty untreated defect as a negative control or a defect filled with autologous bone grafts as a positive control. All groups were evaluated after 4 and 8 weeks of *in vivo* implantation using microcomputed tomography, mechanical testing in flexure, and histomorphometry. It was observed that the use of the wrap resulted in an increased bone volume regenerated when compared to the scaffold-only group (59% greater at 4 weeks and 27% greater after 8 weeks). Additionally, the increase in density of the regenerated bone from 4 to 8 weeks in the wrap group was threefold than that in the scaffold group. The use of the collagen wrap showed significant benefits of increased interfacial bone in-growth (149% greater) and periosteal remodeling (49%) after 4 weeks compared to the scaffold-alone with the two groups being comparable after 8 weeks, by when the collagen membrane showed close-to-complete resorption. While the autograft and wrap groups showed significantly greater flexural strength than the defect group after 8 weeks, the scaffold-alone group was not significantly different from the other three groups. It is most likely that the wrap shows improvement of function by acting like a scaffold for periosteal callus ossification, maintaining the local bone-healing environment while reducing fibrous infiltration (15% less than scaffold only at 4 weeks). This study indicates that the use of a collagen membrane with a hydroxyapatite structural graft provides benefits for bone tissue regeneration in terms of early interfacial integration.

Introduction

The treatment of large-bone defects caused by trauma or disease presents a significant clinical problem. The preferred therapies include the use of autologous grafts, which is limited by availability and associated donor-site morbidity,[1] and structural allografts, which is limited by lack of vascularization and high associated infection risk. These shortcomings have led to extensive research in tissue engineering based on the development of osteoconductive scaffolds with osteoinductive growth factors either codelivered with or to aid in *in situ* recruitment of osteogenic cell sources.[2] The carrier-based delivery of osteoinductive growth factors such as bone morphogenetic proteins (BMPs) (such as infuse collagen graft by Medtronic[3]) has proven to be a promising therapy, but is currently limited by high costs and associated complications, including life-threatening cervical swelling[4] and ectopic bone formation.[5]

Osteoconductive scaffolds are designed to provide a suitable substrate for the in-growth of bone tissue and supporting vasculature and intended to function as space maintainers for bony in-growth.[6] To support the space maintenance function, barrier membranes are used to prevent in-growth of faster growing fibrous tissues in bone defect spaces.[7,8] In a systemic review, it was noted that barrier membranes used in conjunction with bone-grafting

The work was performed at the University of Texas at San Antonio and the U.S. Army Institute of Surgical Research.
[1]Extremity Trauma and Regenerative Medicine Task Area, United States Army Institute of Surgical Research, Fort Sam Houston, Texas.
[2]Department of Biomedical Engineering, The University of Texas at San Antonio, San Antonio, Texas.
[3]College of Dentistry, Chosun University, Gwangju, Republic of Korea.
[4]Institute for Biomaterials Research & Development, Kyungpook National University, Daegu, Republic of Korea.
[5]Department of Orthopaedic Surgery, Columbia University Medical Center, New York, New York.

materials result in improved bone regeneration and repair as compared to grafting materials alone.[9] Guided bone regeneration (GBR), which refers to using barrier membrane guides, has been widely investigated and is widely employed in the treatment of bone defects in maxillofacial surgery, especially to improve the alveolar bone quality before implant placement.[10] While expanded polytetrafluoroethylene membranes were used in the initial development of the technique,[10] resorbable collagen or aliphatic polyester membranes are the most commonly used materials today[11] to eliminate the need for a second surgery for membrane removal. Collagen membranes are preferred owing to their hemostatic function, which leads to early wound stabilization, chemotactic properties toward fibroblasts, and permeability, which facilitates nutrient transport.[12] However, collagen also undergoes fast degradation due to the enzymatic activity of macrophages and leukocytes resulting in poor membrane resistance to collapse.[13] To prevent such collapse from occurring, the membrane guide is either cross-linked for improved mechanical properties[10] or alternately paired with bone grafts or bone graft substitutes within the defect space.[14]

Macroporous calcium phosphates (hydroxyapatite, beta-tricalcium phosphate, and biphasic calcium phosphate) are the most common synthetic bone graft substitutes used with collagen membranes in GBR due to their osteoconductivity and ability to form a direct bond to host bone and to provide a local calcium source for bone regeneration.[14–17] While GBR has been extensively applied, especially in oral and maxillofacial reconstruction, the technology has seen limited use with regard to segmental long-bone defects of the axial skeleton. Additionally, while GBR has been employed with bone chips or calcium phosphate granules, it has rarely been used in conjunction with structural or preformed synthetic grafts. While the use of GBR membranes is essential with bone chips/calcium phosphate granules to prevent migration of these from the defect site, it is not truly essential with structural scaffolds for migration prevention. This raises the question of whether there is any additional benefit to combine the GBR technology with structural scaffolds, especially in the axial skeleton. In this study, we compare a structural porous hydroxyapatite (HAp) graft that we have previously demonstrated to be osteoconductive[18,19] by itself or paired with a collagen membrane guide to investigate the additional benefit of GBR in segmental defects of the rabbit radius. The design hypotheses are that the use of a collagen membrane guide will increase bone regeneration in the defect space,[15] provide a scaffold for the formation of a periosteal callus,[20] and provide a barrier to shield the local regenerative environment.[21]

Materials and Methods

Scaffold preparation

Using a previously described template-coating process, porous fully interconnected HAp scaffolds were prepared. Briefly, polyurethane sponges (EN Murray) of 340-μm mean pore size were used as templates for the scaffolds. The templates were designed to mimic a 10-mm-segmental defect in the rabbit radius model and had an elliptical cross-section to match the explanted bone that averaged a 5-mm major axis and a 3-mm minor axis. The templates were then twice coated in distilled water-based HAp slurry. Binders used with the slurry to improve sintering and to stabilize the scaffold structure included 3% high-molecular-weight polyvinyl alcohol, 1% v/v carboxymethylcellulose, 1% v/v ammonium polyacrylate dispersant, and 3% v/v N,N-dimethylformamide drying agent. Coated sponges were then vacuum-dried overnight before sintering to 1230°C for 3 h in a high-temperature furnace (Thermolyne). All scaffolds were sterilized using ethylene oxide gas sterilization before implantation.

Scaffold characterization

Before animal study, the porosity of the scaffolds was characterized using helium pycnometry (Accupyc 1340) to measure the true solid volume of the scaffold (V_{solid}). Skyscan 1076 (Skyscan, Kontich, Belgium) at an 8.77-μm pixel resolution was used for microcomputed tomography (micro-CT) analysis, and the images were reconstructed using NRecon software (Skyscan). The micro-CT images were thresholded such that the scaffold volume from the micro-CT matched the V_{solid} measured from helium pycnometry. Scaffold porosity, surface-to-volume ratios, and trabecular architectural metrics were determined by three-dimensional morphometric analysis of the images using CTAn software (Skyscan, Kontich, Belgium).

Animal surgery

A unilateral 10-mm-segmental defect was created in the left radial diaphysis of 93 skeletally matured New Zealand White rabbits (Myrtles Rabbitry, Inc., Thompson Station, TN), with minimum of 1 year of age. This study protocol was approved by the Institutional Animal Care and Use Committee at the U.S. Army Institute of Surgical Research. A 20-mm incision was made over the middle third of the radius. The overlying tissues were then dissected to expose the radial diaphysis, where a 10-mm-segmental defect was created with an oscillating saw, under copious irrigation with sterile normal saline (Fig. 1a). The defects had no treatments (negative controls: defect group) or were implanted with autologous bone graft from the iliac crest (positive controls: autograft group) or were alternately implanted with 10-mm scaffolds with uniform trabecular architecture and without (experimental treatments: scaffold group) or with (experimental treatments: wrap group) a collagen membrane guide (Fig. 1b). In the wrap group, postscaffold placement, the collagen wrap (Cytoplast RTM; Ossten, Inc.) was saturated with normal saline and placed around the defect by placing the short axis parallel to the radius and the long axis tucked between bone and muscle to become adjacent to the ulna on both sides, but not extending all the way around (Fig. 1c). Dimensions of the wrap were 20 mm by 30 mm, and placement ensured that 5 mm of wrap overlapped the intact radius portions beyond the proximal and distal defect interfaces. The wrap was then secured in place (stretched snuggly in all directions) with a 2-0 vicryl cerclage suture (tightly tied around the ulna radius complex and wrap) with measures to assure that no vessels or muscles were included (Fig. 1d). A total of two cerclage sutures were used: one on the proximal side and one on the distal side. Due to the existence of a fibro-osseous syndesmosis between the radius and ulna in

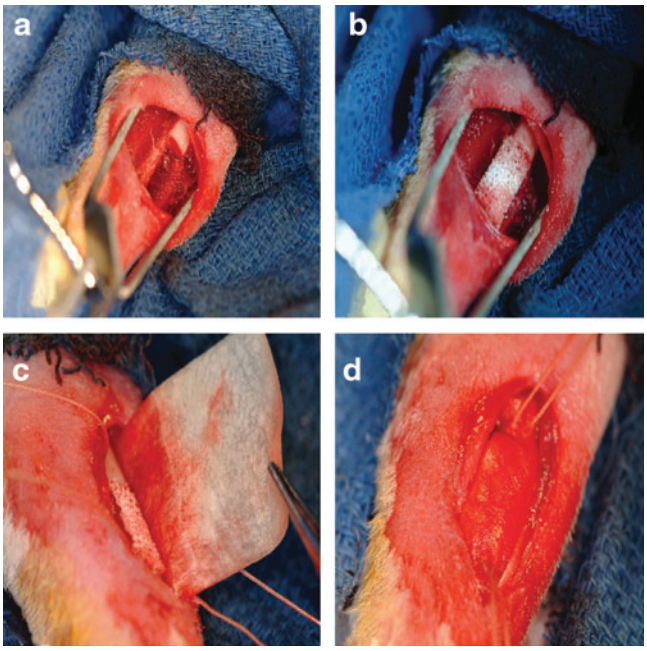

FIG. 1. **(a)** A 10-mm mid-diaphyseal defect was created in the rabbit radius, and experimental treatments included either **(b)** a porous hydroxylapatite scaffold alone or **(c)** with a collagen membrane guide that was **(d)** secured by sutures above and below the defect. Color images available online at www.liebertpub.com/tea

rabbits, no internal or external fixation was necessary in this case. Since no osteoinductive or osteogenic factors were incorporated into the graft substitutes tested (except those inherent in the positive control), a more demanding 20-mm critical-sized defect model[22] was not used, and a healing 10-mm defect model was employed[19] to allow for better characterization of the osteoconductivity of the graft substitutes. Immediately after implantation, the soft tissues were approximated with a continuous 2-0 Vicryl® (Ethicon, Inc.), and the skin was closed with deep dermal stitches using a 3-0 Vicryl (Ethicon, Inc.). Animals were kept alive for 4 weeks ($n=8$ samples/group; $n=7$ samples in wrap group) or 8 weeks ($n=16$ samples/group, $n=14$ samples in wrap group) postsurgery. A power analysis (power = 0.95, $\alpha=0.05$) performed in a parallel study was used to demonstrate that seven animals/group were sufficient to demonstrate significant differences between groups.

Micro-CT evaluation

After euthanasia, all samples were analyzed by micro-CT before histology or mechanical testing. All samples were either wrapped in gauze hydrated with phosphate-buffered saline and preserved frozen for mechanical testing or placed in formalin for histological evaluation, depending on the type of testing after micro-CT evaluation. Micro-CT analysis was performed using Skyscan 1076 at a resolution of 8.77-μm pixel while hydrated. The images were reconstructed using NRecon software to generate grayscale images ranging from 0 to 255, which was equivalent to the density range 0.81–3.34 g/cm^3. The density of the new bone formed in the defect, the average density of the bone in the autograft group, and the density of the regenerated bone formed within the scaffold in the experimental groups while excluding the HAp scaffolds themselves were measured. For this comparison, the tissue density of the ulna in each corresponding group served as a control. The micro-CT-reconstructed axial slices were then evaluated using CTAn software to determine the bone regeneration patterns *in vivo* in terms of growth profiles within the defect site and overall bone volume. New bone evaluation was based on density differences between scaffold (2.5 g/cm^{3}mean) and newly forming osteoid or remodeling native bone (1.2–1.7 g/cm^3). While the HAp scaffold could be separated in micro-CT evaluation from the regenerated bone, this was not possible for the autograft group, and all the data reported for that group included both the regenerated bone as well as the remodeled autograft. The region of interest was a 3D volume that extended over the 10-mm defect space created at the time of surgery. The bone area in each 8.77-μm section of this 10-mm defect space was computed for all four treatments to observe the trends in bone regeneration along the length of the defect, from the proximal to the distal interface with the host bone. Total bone formed within the defect spaces was also measured, which included the calcified interosseous syndesmosis, but excluded the ulna.

Histological evaluation

Immediately after euthanasia, eight excised radii and ulnae per group (seven for the wrap group) were fixed in formalin and then subjected to a dehydration and infiltration method (Exakt) for 14 days via a tissue processer (Leica TP1020 System). Samples were next embedded in photocuring resin (Technovit 7200 VLC) and polymerized under blue light for 24 h. Block samples were adhered to a parallel plexiglass slide using the Exakt 7210 VLC system. Radial sections of the sample were then cut (200–300 μm) using a diamond-precision parallel saw (Exakt-Apparatebau Hermann). The cut slides were subjected to grinding (50–100 μm) and polishing (Exakt 400 CS, AW 110) and stained for both connective tissue (paragon), calcium (alizarin red), and collagen type I (aniline blue).

Histomorphometric analysis was then used to quantify the data using Bioquant Osteo. The basic measurement arrays were bone area inside scaffold, original ulna area, periosteal remodeling of the ulna, bone area outside scaffold, and scaffold area. Periosteal remodeling was calculated as a percentage increase in the original ulna area. New bone refers to new or remodeled bone that includes bone area inside scaffold, periosteal ulna area, and bone area outside scaffold. Paragon selective for noncollagen connective tissue was used in contrast with aniline blue staining of collagen to differentiate the fibrous connective tissue from osteoid. The separation in stained areas was confirmed using polarized light microscopy to ensure no overlap of paragon-stained fibrous tissue with birefringence of collagen type I. The fibrous tissue area infiltration to total area was measured based on color mapping in BioquantOsteo to select the area of fibrous versus collagen zones.

Biomechanical evaluation

Immediately after euthanasia, eight excised radii and ulnae per group (seven for the wrap group) were used for mechanical testing. The radius and ulna were cut to a 26-mm

length centered about the defect while preserving the interosseous membrane. The corresponding site on the intact contralateral limb was excised to serve as controls for the biomechanical evaluation. The specimens were tested to flexural failure in a 4-point bending configuration with 10-mm spacing between the loading supports and 20-mm spacing between the base supports. The specimens were loaded in dorsal–ventral orientation at a constant strain rate of 0.5 mm/min on an Insight 5 uniaxial test frame (MTS Systems Corp.). Flexural modulus and peak flexural strength were measured, and flexural toughness was computed as the total energy observed. The moment of inertia of the specimen was calculated from the micro-CT images using the CTAn software package.

Statistical analysis

All data are reported as mean ± standard error of the mean. Significance in histological, micro-CT, and mineral density measures reported was determined using a two-way analysis of variance (ANOVA) and Tukey's test for *post hoc* evaluation. Significance in biomechanical evaluations was determined using a one-way ANOVA and Tukey's test for *post hoc* evaluation. The significance level was set at $p < 0.05$ for all statistical measures reported.

Results

Scaffold characterization

The scaffolds used in this study had a mean scaffold porosity of 65.5% ± 4.5% as indicated by the helium pycnometry and corroborated by the micro-CT analysis (65.48% ± 4.7%). The micro-CT morphometric analysis also indicated that the trabecular thickness of the scaffolds was 209 ± 7 μm; the trabecular spacing, which corresponds to the pore size, was 440 ± 40 μm, and the scaffold surface-to-volume ratio was 16.9 ± 1.3 mm^{-1}.

Micro-CT evaluation

The longitudinal reconstructions of the rabbit forearm after 4 and 8 weeks *in vivo* are shown in Figure 2 for all four treatment groups. The defect group shows the existence of three distinct fronts of bone formation in the segmental radius defect model: conical fronts of ossification stemming from the proximal and distal cortical bone interfaces of the defect and the ossification and ingrowth from the interosseous syndesmosis that connects the ulna to the radius in the rabbit. Bone formation from the interfaces and syndesmosis into the scaffolds was also observed in both the scaffold-only and wrap groups. In the autograft group, a robust regeneration response was observed within the defect space, but the implanted autograft particles could still be distinguished at 4 weeks, whereas far more remodeling of the ossification was observed at 8 weeks, and individual implanted cortical fragments could no longer be distinguished within the new bone.

Quantitative differences in the spatial patterns of bone regeneration after 4 and 8 weeks of *in vivo* implantation are shown in Figure 3, which shows the regenerated bone distribution from the proximal to the distal interface for all four groups. The width of the bands in Figure 3 corresponds to variations in bone regeneration at each axial location between different samples within a group. At 4 weeks, a large variation was observed in bone regeneration at axial locations within the autograft group (mean standard error 1.85 mm^3, compared to 0.52–0.80 mm^3 for the other three groups, $p < 0.001$), which can be attributed to the differences in distribution of pulverized autograft across the defect space between different animals in the group. The wrap group showed significantly greater bone regeneration than the scaffold group at both the proximal and distal interfaces (within 1 mm from each interface, $p < 0.024$). While the regenerated bone at the interfaces of the empty defect group was similar to that seen in the scaffold group, the bone regenerated over the interior defect space (central 8-mm region) was significantly lower (Fig. 3a,

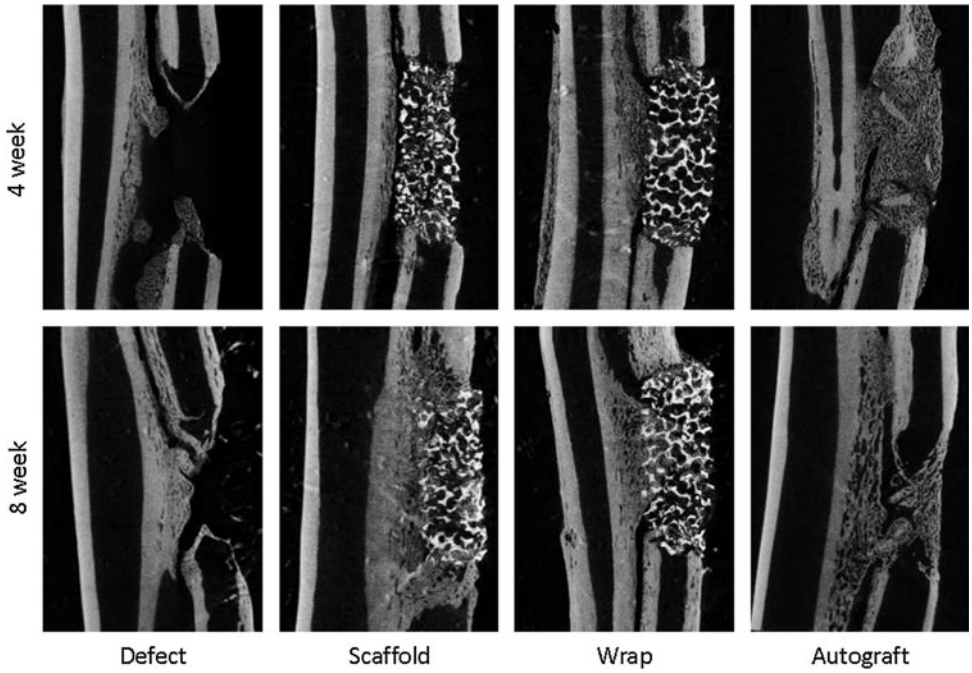

FIG. 2. Microcomputed tomography evaluation showing bone regeneration and remodeling in the defect, scaffold, wrap, and autograft groups after 4 or 8 weeks *in vivo* shown in coronal longitudinal sections through the rabbit forearm.

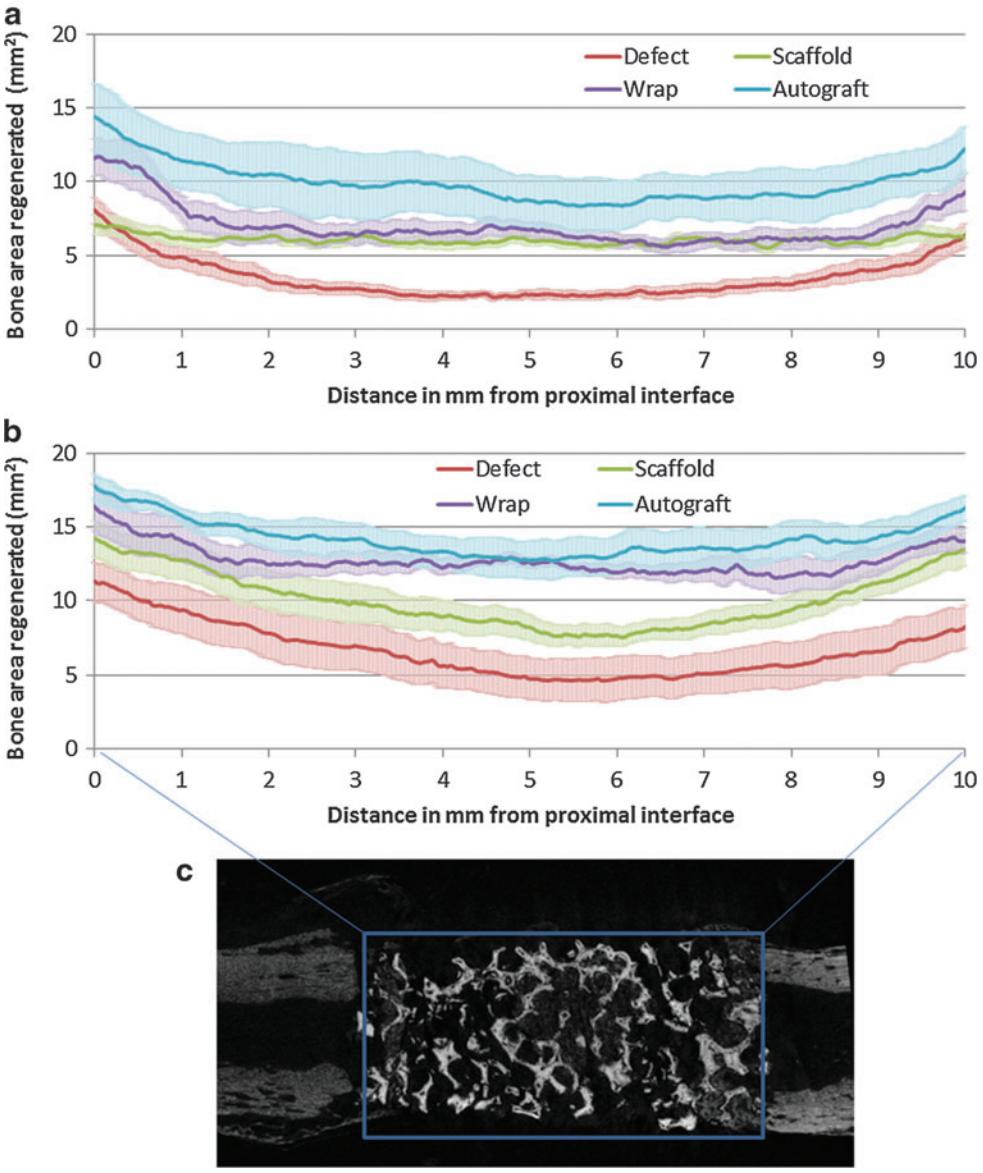

FIG. 3. The cross-sectional regenerated bone (excluding ulna and scaffold) area (mean ± SEM) was plotted every 8.7 μm across the 10-mm space **(c)** created from the proximal (0 mm) to the distal (10 mm) interface to assess spatial bone regeneration and remodeling trends for the four treatment groups after **(a)** 4 and **(b)** 8 weeks *in vivo* implantation. Color images available online at www.liebertpub.com/tea

$p < 0.001$) than the bone regenerated in the scaffold group in the same space. After 8 weeks, the overall regenerated bone volume remained in the same order as observed after 4 weeks: autograft > wrap > scaffold > defect (Fig. 3b). At 8 weeks, all four groups indicated trends of greater bone formation at the interfaces as opposed to the center of the defect. Within the wrap group, the bone formation at the center of the defect space was significantly greater than the scaffold group, while still lesser than the autograft group. The empty defect group showed the least bone regenerated at every location within the defect space after 8 weeks compared to the other three groups.

The tissue mineral density of the regenerated and remodeled bone within the 10-mm defect site in the radius for all four groups at both 4 and 8 weeks and normalized to the tissue mineral density of the corresponding 10-mm length of ulna is reported in Figure 4 as the relative mineral density. The defect, scaffold, and wrap groups all showed an increase in the relative density from 4 to 8 weeks, whereas no change was observed in the autograft group. This suggests that there is primarily a remodeling response in the autograft group rather than a pure regenerative response as observed in the other groups. Both the defect and scaffold-only groups showed a significantly lower relative mineral density at 4 weeks than the autograft group ($p < 0.05$), while the relative mineral density of the wrap group did not show a significant difference at 4 weeks. Additionally, while the relative mineral density of the scaffold-only group was significantly lower than all other groups after 8 weeks ($p < 0.05$), the defect, wrap, and autograft groups were comparable after 8 weeks *in vivo* implantation.

The micro-CT evaluation of regenerated bone volume (Fig. 5) indicated that while the volume of bone regenerated within the scaffold in both the scaffold-only and wrap groups was comparable at both 4 and 8 weeks, the ossified bone volume in the surrounding callus was significantly greater for the wrap group compared to the scaffold-only group ($p < 0.05$). The total regenerated bone volume in the wrap group (excluding the volume of the scaffold itself) was

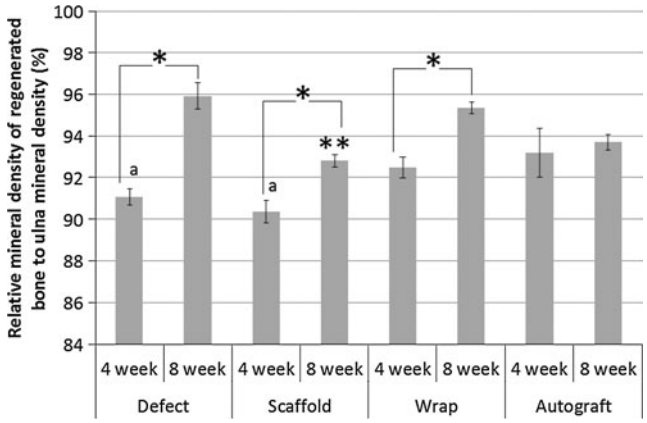

FIG. 4. The relative mineral density of the regenerated bone was calculated by normalizing to ulna mineral density. All groups, except the autograft, showed an increase from 4 to 8 weeks (*). The autograft showed a greater relative density at 4 weeks than the defect and scaffold **(a)**, while the scaffold showed the least relative density at 8 weeks (**).

comparable to the total bone volume in the autograft group (including implanted autograft) after both 4 and 8 weeks and was significantly greater than both the defect and scaffold-only groups at either time point (Fig. 5).

Histological evaluation

Representative radial sections after histological processing and staining for connective tissue and mineralized tissue are shown in Figure 6 for all four groups after 4 and 8 weeks of *in vivo* implantation. Since the histological evaluation was performed at the defect interfaces, these images are representative of interfacial bony regeneration. Hollow conical bone growth fronts were observed to regenerate into the defect space from both the native cortical interfaces adjacent to the defect space, most clearly observed in the empty defect, but also in the scaffold, wrap, and autograft groups. All groups showed clearly greater bone formation after 8 weeks when compared to the 4-week samples. After 8 weeks, a clear cortex-like reorganization of bone on the periphery of the defect space was observed, especially in the wrap and autograft groups (labeled C in Fig. 6). While remnants of the collagenous wrap were observed after 4 weeks as fragments, these were mostly resorbed and not distinctly identifiable around the defect space after 8 weeks *in vivo*. A periosteal ossification response was observed on the periphery of the ulna in all groups, especially on the surface toward the radius (labeled P in Fig. 6). This was specifically quantified in the histomorphometric analysis (Table 1), and it was observed that at 4 weeks, the wrap group showed significantly greater periosteal remodeling of the ulna when compared to the scaffold group ($p < 0.05$). After 8 weeks, both the wrap and the scaffold groups showed significantly greater periosteal remodeling than the defect group, with the autograft group being intermediate to the defect group and the scaffold and wrap groups. The empty defect group showed the greatest fibrous tissue infiltration within the defect space after both 4 and 8 weeks. Both the wrap and autograft groups showed significantly lesser fibrous tissue within the defect space after 4 weeks than the scaffold group without wrap ($p < 0.05$). No differences between the fibrous tissue in the scaffold, wrap, and autograft groups were observed after 8 weeks, and the extent of fibrous tissue in-growth significantly reduced in the scaffold group between weeks 4 and 8. In terms of bone volume-to-tissue volume ratio at the interfaces, no significant differences were observed between the defect, scaffold, and wrap groups histologically. The total new bone area (total regenerated or remodeled bone within the scaffold, in the ossified scaffold callus or periosteal ossification) within the wrap group was significantly greater than the scaffold group after 4 weeks ($p < 0.05$). The new bone area in both the wrap and scaffold groups was similar at 8 weeks, but significantly greater than the defect group ($p < 0.05$). The autograft group showed significantly greater new bone area and bone-to-tissue volume ratio after both 4 and 8 weeks *in vivo* than the other three groups ($p < 0.01$).

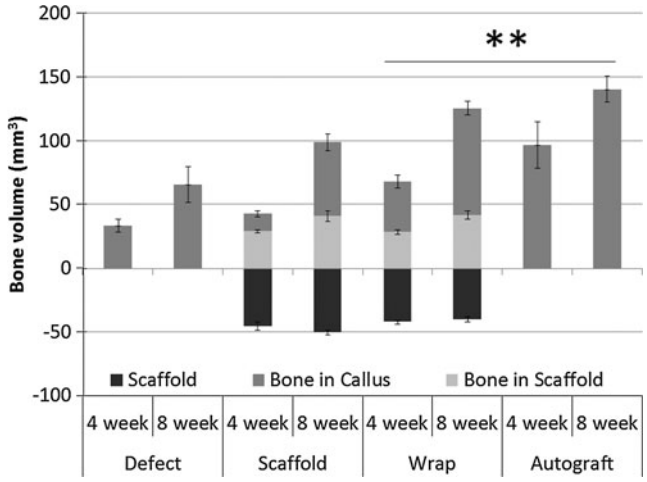

FIG. 5. The total volume of the scaffold and the volume of regenerated bone within the scaffold and in the callus around the scaffold in the scaffold and wrap treatment groups were calculated at both 4 and 8 weeks and compared to the total bone volume in the defect and autograft treatments. Total regenerated bone is significantly greater (**) in the wrap and autograft group after both 4 and 8 weeks compared to the scaffold and empty defect group.

Biomechanical evaluation

As shown in Table 2, the flexural testing of the rabbit radius–ulna complex after 8 weeks revealed that both the wrap and autograft groups showed significantly stronger flexural strength than the defect group, whereas the scaffold group did not. Also, the flexural strength of the experimental limb (with treatment) in the wrap group was observed to be significantly higher than the untreated contralateral limb. The flexural modulus of the defect group experimental limb was significantly lower than its contralateral control. The flexural modulus of the wrap treatment was also significantly higher than the defect treatment group ($p < 0.05$). The flexural toughness of the scaffold, wrap, and autograft treatments was significantly greater than the toughness of the defect treatment. However, it was only in the wrap and autograft groups that the flexural toughness of the experimental limb was significantly greater than the respective

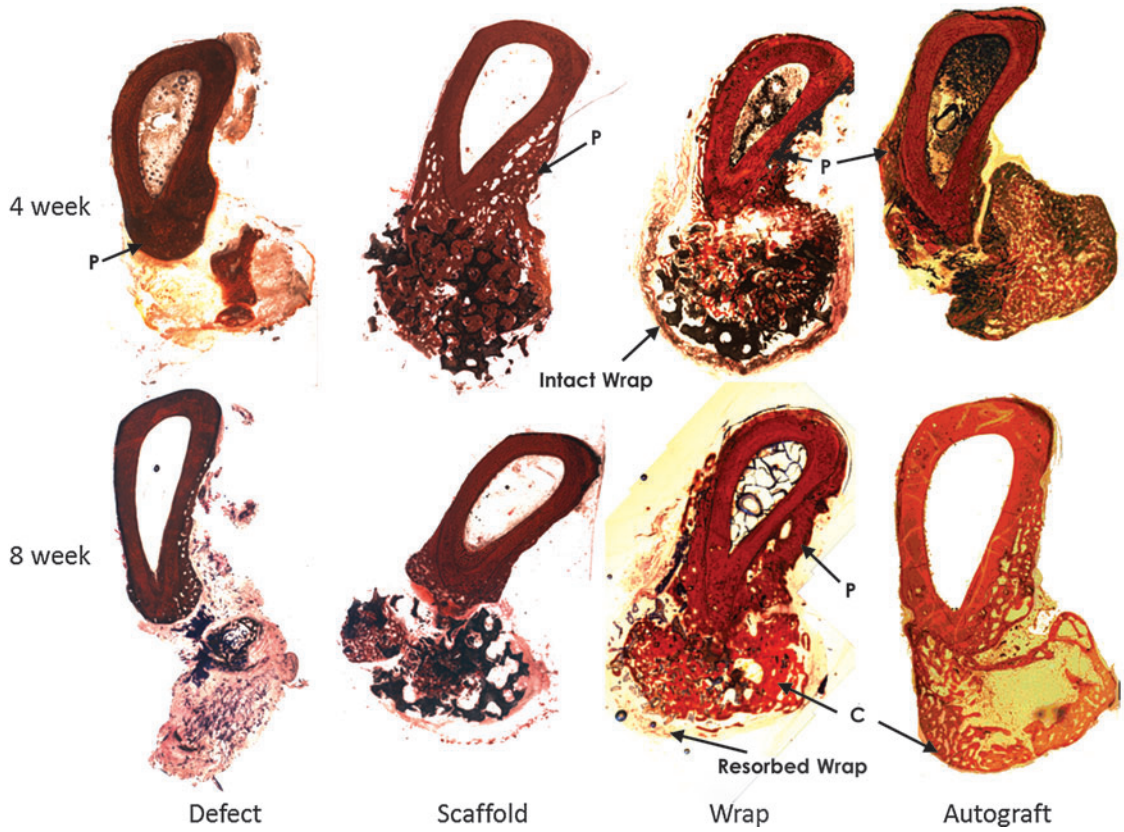

FIG. 6. Bone tissue cross-sections at 4 and 8 weeks postsurgery and stained with Paragon for connective tissue (violet) and alizarin red for mineralized bone tissue (red), showing very little bone formation and significant connective tissue in the defect; regeneration and bone growth infiltrating the scaffold (black) in the scaffold and wrap groups and a robust regeneration response are seen in the autograft treatment. Resorption of the collagen membrane is seen from 4 (intact wrap) to 8 weeks (resorbed wrap) in the wrap group; periosteal remodeling of the ulna (labeled P) is also observed in all groups, and cortical-like bone fronts (labeled C) were observed in the wrap and autograft groups.

contralateral control limb. Four of the eight samples in the scaffold and one of the seven samples in the wrap experimental groups failed at the scaffold–bone interface. The remainder of each group failed via a short oblique fracture through the intact portion of the radius away from the defect site. Additionally, failure of the ossified interosseous membrane was observed in five of the eight samples in the scaffold group and all seven samples in the wrap group. All samples in the empty defect group failed by a short oblique fracture of the ulna (three within the defect space and five away from the defect space). The defects treated with autograft failed via a short oblique crack at the graft interface in six out of the eight samples tested and the other two failed at the interosseous membrane.

Discussion

Tissue-engineering approaches toward regenerating bone have long been based on the pairing of osteoconductive scaffolds with osteoinductive factors and osteogenic cells in a

Table 1. Area Measurements from Histomorphometric Analysis of Bone Regeneration in the Defect, Scaffold, Wrap, and Autograft Groups at the Defect Interfaces After 4 and 8 Weeks *In Vivo*

	Defect		*Scaffold*		*Wrap*		*Autograft*	
	4 week	*8 week*	*4 week*	*8 week*	*4 week*	*8 week*	*4 week*	*8 week*
Bone/total tissue (%)	21.8±6.8	15.7±7.0	12.3±2.5	32.5±7.4[a]	25.6±7.8	26.0±5.5	77.0±6.5[b]	63.0±7.8[b]
Fibrous/total tissue (%)	71.0±6.1[b]	73.0±7.5[b]	49.2±1.5	37.8±4.0[a]	34.6±3.9[c]	33.3±1.7	22.4±6.1[c]	34.7±7.1
New bone area (mm^2)	7.9±1.6	5.1±1.1	4.1±0.3	12.7±2.0[a,d]	10.1±1.5[c]	13.6±1.2[d]	19.7±2.0[b]	22.5±1.2[b]
Periosteal remodeling of the ulna (%)	56±12	33±5	32±5	97±17[a,d]	81±12[c]	104±13[d]	45±6	72±8

[a]A significant increase from 4 to 8 weeks.
[b]Significant differences from all other groups.
[c]Significant differences from the scaffold group.
[d]Significant differences from the defect group.

Table 2. Flexural Mechanical Strength, Modulus, and Toughness of the Rabbit Forearm Measured in 4-Point Bending and Presented as a Comparison Between the Experimental Side Where the Surgery Was Performed and the Contralateral Arm as a Control

	Flexural strength (MPa)		*Flexural modulus (MPa)*		*Flexural toughness (MPa)*	
	Experimental	*Contralateral*	*Experimental*	*Contralateral*	*Experimental*	*Contralateral*
Defect	16.1 ± 2.8	20.5 ± 2.2	489 ± 97[a]	826 ± 75	41.6 ± 6.1	71.2 ± 8.6
Scaffold	36.0 ± 4.3	23.9 ± 2.7	748 ± 110	636.5 ± 66.6	203.7 ± 27.3[b]	123.7 ± 29.6
Wrap	49.1 ± 9.7[a,b]	26.7 ± 3.2	1015 ± 97[b]	881 ± 108	228.1 ± 43.2[a,b]	117.2 ± 20.4
Autograft	43.8 ± 5.4[b]	33.1 ± 3.8	796 ± 68	750 ± 82	246.0 ± 40.2[a,b]	140.3 ± 33.3

[a]A significant difference between experimental and contralateral controls.
[b]Significant differences from the defect group.

suitable mechanical environment.[23] In this study, we evaluate a strategy to improve the regenerative capacity of structural osteoconductive grafts by using a permeable, resorbable membrane guide with no additional osteogenic or osteoinductive factors in a long-bone defect model. It was found that the use of a collagen membrane guide in conjunction with an open porous hydroxyapatite scaffold significantly increased the total bone volume regenerated after both 4 and 8 weeks of *in vivo* implantation compared to using the hydroxyapatite scaffold alone. The total bone volume regenerated when using the wrap, the flexural strength and toughness after 8 weeks and the density of the regenerated bone mineral were all comparable to autologous bone grafts, which are the gold standard of care for large-bone defects. A group pairing the autologous bone graft with a collagen membrane guide was not included in this study, because previous investigations in the mandible defects of beagle dogs have shown no difference in the bone regeneration achieved when using autologous bone chips with or without a collagen membrane.[16]

Unlike maxillofacial defects where the primary objective is not only to restore volume and contour[15] but to also support osseo-integrated implant placement postbone regeneration, the primary objective in long-bone defects of the extremities is to regenerate weight-bearing bones with appropriate mechanical functionality. From the flexural testing to failure conducted in this study, it was observed that the flexural strength, modulus, and toughness of the wrap treatment were all significantly greater than the untreated defect group and comparable with no significant differences from the autograft treatment. Further, unlike calcium phosphate granules, which have been widely used in conjunction with GBR previously,[14,15,20] a preformed structural hydroxyapatite graft was used in this study that possibly allowed for load transfer across the defect space from the time implant placement. It has been previously speculated that insufficient mechanical protection provided by the membrane when used in conjunction with granules led to micromotion and successively the formation of fibrous encapsulation.[16] However, the use of a preformed graft, which is seen to be osteoconductive over the duration of the study in the scaffold-only group, eliminates the need for the membrane to act as a structural containment for the graft. Additionally, the membrane does function as a barrier to the faster-growing connective tissue cell populations that lead to fibrous encapsulation as previously observed[24] and was seen to resorb over the duration of the study with fragmentation observed after 4 weeks and almost complete resorption by 8 weeks. This was supported by significantly lesser fibrous tissue observed within the defect after 4 weeks when using the barrier membrane and comparable fibrous tissue in groups with and without the barrier membrane at 8 weeks by when close-to-complete resorption of the collagen membrane was observed. When taken in conjunction with observations that greater interfacial bone regeneration was observed with a collagen wrap after 4 weeks when compared to the scaffold alone, this study suggests that the trend of greater strength might stem from an early bone regeneration response, and better results of mechanical stability might have been observed with a slower-degrading membrane guide.

The periosteum forms a major source of osteogenic cells in the healing of segmental bone defects, and the collagen membrane guide has been suggested to be effective primarily, since it acts as a scaffold to maintain periosteal continuity.[14] Similar to previous reports,[14,20] we observed periosteal callus-like tissue formation and successive ossification around the collagenous wrap. This was observed from the micro-CT analysis as a significant early increase in callus bone volume in the wrap group compared to the scaffold-alone group at 4 weeks, which was sustained at 8 weeks. Additionally, the histomorphometric analysis at the interfaces also indicated significantly greater periosteal ossification in the wrap group compared to the scaffold-only group. Unlike the previous studies[14,20] that used bone marrow grafts in addition to the collagen membrane guide and calcium phosphate granules, no additional osteogenic or osteoinductive factor was included in this study. Both hydroxyapatite[17,25] and collagen[26,27] have been widely used for the delivery of a variety of growth factors to enhance bone regeneration. The formation of ectopic bone has been a concern with the use of recombinant human BMP-2 clinically,[5] but reports suggest that the use of vascularized periosteal flaps reduced the occurrence of heterotopic ossification associated with BMP-2 delivery,[28] indicating that collagenous barrier membranes might function in a similar fashion. It is also possible that the ability of these membranes to better preserve a suitable osteogenic fracture-healing environment might also lead to better retention of delivered growth factors and improved efficacy at lower doses. Thus, the collagen membrane guide paired with a hydroxyapatite scaffold forms an improved osteoconductive substrate for further incorporation of osteoinductive factors or the delivery of osteogenic cells. However, since complete bridging of the defect space was not observed in this study at 8 weeks

while resorption of the collagen guide was observed, results suggest the need to develop collagen guides with longer degradation times to match *in vivo* bone regeneration rates.

Conclusions

The additional use of a collagen membrane guide significantly improved early interfacial bone regeneration compared to the use of a preformed hydroxyapatite porous graft alone in the absence of additional osteoinductive or osteogenic factors. The use of the collagen guide and hydroxyapatite graft was seen to result in more uniform bone volume regeneration across the long-bone defect site in rabbits and was a comparable synthetic alternative to autologous bone grafts in all metrics measured in this study.

Acknowledgments

This study was supported in part by the Department of Defense funds and the Orthopaedic Extremity Trauma Research Program grants (USAMRMC # W81XWH-08-1-0393 and W81XWH-07-1-0717). The opinions or assertions contained herein are the private views of the author and are not to be construed as official or as reflecting the views of the Department of the Army or the Department of Defense. This study has been conducted in compliance with the Animal Welfare Act, the implementing Animal Welfare Regulations, and in accordance with the principles of the Guide for the Care and Use of Laboratory Animals.

Disclosure Statement

No competing financial interests exist.

References

1. Mauffrey, C., Madsen, M., Bowles, R.J., and Seligson, D. Bone graft harvest site options in orthopaedic trauma: a prospective *in vivo* quantification study. Injury **43,** 323, 2012.
2. Giannoudis, P.V., Dinopoulos, H., and Tsiridis, E. Bone substitutes: an update. Injury **36,** S20, 2005.
3. McKay, W., Peckham, S., and Badura, J. A comprehensive clinical review of recombinant human bone morphogenetic protein-2 (INFUSE® Bone Graft). Int Orthop **31,** 729, 2007.
4. Tumialan, L.M., and Rodts, G.E. Adverse swelling associated with use of rh-BMP-2 in anterior cervical discectomy and fusion. Spine J **7,** 509, 2007.
5. Axelrad, T.W., Steen, B., Lowenberg, D.W., Creevy, W.R., and Einhorn, T.A. Heterotopic ossification after the use of commercially available recombinant human bone morphogenetic proteins in four patients. J Bone Joint Surg Br **90-B,** 1617, 2008.
6. Carlo Reis, E.C., Borges AaPB, Araujo, M.V.F., Mendes, V.C., Guan, L., and Davies, J.E. Periodontal regeneration using a bilayered PLGA/calcium phosphate construct. Biomaterials **32,** 9244, 2011.
7. Aaboe, M., Pinholt, E.M., Hjørting-Hansen, E., Solheim, E., and Praetorius, F. Guided tissue regeneration using degradable and nondegradable membranes in rabbit tibia. Clin Oral Implants Res **4,** 172, 1993.
8. Queiroz, T.P., Hochuli-Vieira, E., Gabrielli, M.A., and Cancian, D.C. Use of bovine bone graft and bone membrane in defects surgically created in the cranial vault of rabbits. Histologic comparative analysis. Int J Oral Maxillofac Implants **21,** 29, 2006.
9. Sculean, A., Nikolidakis, D., and Schwarz, F. Regeneration of periodontal tissues: combinations of barrier membranes and grafting materials–biological foundation and preclinical evidence: a systematic review. J Clin Periodontol **35,** 106, 2008.
10. von Arx, T., Broggini, N., Jensen, S.S., Bornstein, M.M., Schenk, R.K., and Buser, D. Membrane durability and tissue response of different bioresrbable barrier membranes: a histologic study in the rabbit calvarium. Int J Oral Maxillofac Implants **20,** 843, 2005.
11. Hutmacher, D., Hurzeler, M.B., and Schliephake, H. A review of material properties of biodegradable and bioresorbable polymers and devices for GTR and GBR applications. Int J Oral Maxillofac Implants **11,** 667, 1996.
12. Schwarz, F., Rothamel, D., Herten, M., Wüstefeld, M., Sager, M., Ferrari, D., *et al.* Immunohistochemical characterization of guided bone regeneration at a dehiscence-type defect using different barrier membranes: an experimental study in dogs. Clin Oral Implants Res **19,** 402, 2008.
13. Schwarz, F., Herten, M., Ferrari, D., Wieland, M., Schmitz, L., Engelhardt, E., *et al.* Guided bone regeneration at dehiscence-type defects using biphasic hydroxyapatite-beta tricalcium phosphate (Bone Ceramic®) or a collagen-coated natural bone mineral (BioOss Collagen®): an immunohistochemical study in dogs. Int J Oral Maxillofac Surg **36,** 1198, 2007.
14. Jegoux, F., Goyenvalle, E., Cognet, R., Malard, O., Moreau, F., Daculsi, G., *et al.* Mandibular segmental defect regenerated with macroporous biphasic calcium phosphate, collagen membrane, and bone marrow graft in dogs. Arch Otolaryngol Head Neck Surg **136,** 971, 2011.
15. Benque, E., Zahedi, S., Brocard, D., Marin, P., Brunel, G., and Elharar, F. Tomodensitometric and histologic evaluation of the combined use of a collagen membrane and a hydroxyapatite spacer for guided bone regeneration: a clinical report. Int J Oral Maxillofac Implants **14,** 258, 1999.
16. Jung, R.E., Lecloux, G., Rompen, E., Ramel, C.F., Buser, D., and Hammerle, C.H.F. A feasibility study evaluating an *in situ* formed synthetic biodegradable membrane for guided bone regeneration in dogs. Clin Oral Implants Res **20,** 151, 2009.
17. Guda, T., Appleford, M., Oh, S., and Ong, J.L. A cellular perspective to bioceramic scaffolds for bone tissue engineering: the state of the art. Curr Top Med Chem **8,** 290, 2008.
18. Appleford, M.R., Oh, S., Oh, N., and Ong, J.L. *In vivo* study on hydroxyapatite scaffolds with trabecular architecture for bone repair. J Biomed Mater Res A **89,** 1019, 2009.
19. Guda, T., Walker, J.A., Pollot, B.E., Appleford, M.R., Oh, S., Ong, J.L., *et al. In vivo* performance of bilayer hydroxyapatite scaffolds for bone tissue regeneration in the rabbit radius. J Mater Sci Mater Med **22,** 647, 2011.
20. Jégoux, F., Goyenvalle, E., Cognet, R., Malard, O., Moreau, F., Daculsi, G., *et al.* Reconstruction of irradiated bone segmental defects with a biomaterial associating MBCP+®, microstructured collagen membrane and total bone marrow grafting: An experimental study in rabbits. J Biomed Mater Res Part A **91A,** 1160, 2009.
21. He, H., Huang, J., Chen, G., and Dong, Y. Application of a new bioresorbable film to guided bone regeneration in tibia defect model of the rabbits. J Biomed Mater Res Part A **82A,** 256, 2007.
22. Bakker, A.D., Schrooten, J., van Cleynenbreugel, T., Vanlauwe, J., Luyten, J., Schepers, E., *et al.* Quantitative screening of engineered implants in a long bone defect model in rabbits. Tissue Eng Part C Methods **14,** 251, 2008.

23. Giannoudis, P.V., Einhorn, T.A., and Marsh, D. Fracture healing: the diamond concept. Injury **38 Supplement 4,** S3, 2007.
24. Schlegel, A.K., Möhler, H., Busch, F., and Mehl, A. Preclinical and clinical studies of a collagen membrane (Bio-Gide®). Biomaterials **18,** 535, 1997.
25. Son, J.S., Appleford, M., Ong, J.L., Wenke, J.C., Kim, J.M., Choi, S.H., *et al.* Porous hydroxyapatite scaffold with three-dimensional localized drug delivery system using biodegradable microspheres. J Control Release **153,** 133, 2011.
26. Matsumoto, A., Yamaji, K., Kawanami, M., and Kato, H. Effect of aging on bone formation induced by recombinant human bone morphogenetic protein-2 combined with fibrous collagen membranes at subperiosteal sites. J Periodontal Res **36,** 175, 2001.
27. Takayama, Y., and Mizumachi, K. Effect of lactoferrin-embedded collagen membrane on osteogenic differentiation of human osteoblast-like cells. J Biosci Bioeng **107,** 191, 2009.
28. Vogelin, E., Jones, N.F., Huang, J.I., Brekke, J.H., and Lieberman, J.R. Healing of a critical-sized defect in the rat femur with use of a vascularized periosteal flap, a biodegradable matrix, and bone morphogenetic protein. J Bone Joint Surg Am **87,** 1323, 2005.

Address correspondence to:
Teja Guda, PhD
Department of Biomedical Engineering
The University of Texas at San Antonio
One UTSA Circle
San Antonio, TX 78249

E-mail: teja.guda@gmail.com

Received: January 31, 2012
Accepted: July 24, 2012
Online Publication Date: September 14, 2012